


Novel eugenol-based antimicrobial coatings on aluminium substrates for food packaging applications

Elena Orlo¹ | Mariamelia Stanzione² | Margherita Lavorgna¹ |
 Marina Isidori¹ | Aldo Ruffolo³ | Ciro Sinagra³ | Giovanna G. Buonocore²  |
 Marino Lavorgna²

¹University of Campania “Luigi Vanvitelli”, Via Vivaldi 43, Caserta, Italy

²Institute of Polymers, Composites and Biomaterials – CNR, Portici (Naples), Italy

³Laminazione Sottile S.p.A., San Marco Evangelista, Caserta, Italy

Correspondence

Margherita Lavorgna, University of Campania “Luigi Vanvitelli”, Via Vivaldi 43, 81100 Caserta, Italy.

Email: margherita.lavorgna@unicampania.it

Giovanna G. Buonocore, Institute of Polymers, Composites and Biomaterials – CNR, P.le E. Fermi 1, 80055 Portici (Naples), Italy.

Email: giovannagiuliana.buonocore@cnr.it

Abstract

Active packaging systems, interacting directly with the enclosed food, can delay or inhibit those phenomena responsible for food quality decay, contributing to the food shelf-life extension. In this work a vinyl resin-based coating containing free or loaded eugenol (EG) in Santa Barbara Amorphous (SBA)15 mesoporous silica nanoparticles is designed to coat flexible aluminium foils to obtain an antimicrobial material. Thermogravimetric analysis shows a good loading capacity of eugenol in SBA15 (48% wt/wt). SEM analysis shows a good dispersion of free EG in the hosting polymeric matrix, whereas some EG/SBA15 particles aggregations are observed in the material. Water contact angle highlights a higher hydrophobicity of the eugenol based-materials ($>90^\circ$) compared to the pristine vinyl coating (85°). Electrochemical impedance spectroscopy highlights no corrosion phenomena of the VIN/5%(EG/SBA15_{EG}) coating and corrosion phenomena of the VIN/5%EG coating after 7 days of exposure to lactic acid pH = 4. Finally, the two active coatings are studied to evaluate their antibacterial activity using the ISO 22196. Interestingly, results demonstrate that when eugenol is loaded in the SBA15 mesoporous silica nanoparticles the antimicrobial activity of the material significantly increases against both foodborne pathogens and food spoilage bacteria, achieving the highest microbial growth reduction on *S. aureus* ($R = 3.62$ log).

KEYWORDS

aluminium substrates, antimicrobial coatings, essential oils, mesoporous silica nanoparticles, resins

1 | INTRODUCTION

The development and the design of active films characterized by specific features, such as antimicrobial and antioxidant properties, with potential applications as wrapping or coating for foods, has become a worldwide challenge over the past few decades.¹ To avoid the food quality decay, active packaging can directly interact with the enclosed

food by delaying or inhibiting the mold or bacteria growth, concurring to achieve shelf-life extension.²

Coating technology is one of the main commonly used techniques, consisting of a plastic film with enhanced functionality attained by applying a liquid dispersion, usually resin and solvent based, onto the packaging systems.³ The coating formulation can be applied at room temperature, and it needs only a flash of hot air, no

higher than 40°C, to allow the solvent to evaporate, avoiding the loss of the initially added active compound.

Active agents (e.g., oxygen scavengers, antioxidants, antimicrobials, enzymes) can be incorporated into coatings to develop active packaging by using several techniques involving different mechanisms, either migratory, in which the active agent is capable to migrate into the enveloped food (i.e. embedding, non-covalent immobilization) and non-migratory, where the active agent is trapped into the packaging matrix or onto its surface (covalent immobilization, some layer-by-layer deposition techniques, photografting).⁴

Encapsulation of essential oils, as natural antioxidant and antimicrobial compounds, into food packaging systems has been studied and industrially developed to implement the coating technology.^{5–7} Coating technology additional advantage is its feasibility for different material substrates, such as paper, board, plastics and aluminium or their combinations, either as single materials or multilayers, either rigid and flexible materials.

Some of aluminium foil applications in food packaging, as an uncoated metal and/or in combination with other materials include cans, sheets, films, trays, tins, containers. This material, very light but strong, can be obtained and converted into complex shapes, characterized by an excellent corrosion temperature resistance, a high thermal and electrical conductivity, and it can be also recycled without lessening the quality. Moreover, its barrier efficiency against light, moisture, volatile aroma, as well as oxygen and other gases, is generally higher than any plastic laminate materials.¹ Bare aluminium foils are mainly used as household foil, wrappings and trays, but today aluminium can no longer be considered chemically inert.⁸ In fact, its contact with highly acidic or alkaline products and salts induces a surface leaching which leads to the migration of aluminium particles to the enveloped foodstuff.⁹ In the case of aluminium ingestion at high concentrations into the organism, due to contaminated food, it can cause serious damage to human health.¹⁰ In this regard, recent studies have revealed that aluminium toxicity could lead to Alzheimer's and other human neuro-degenerative diseases.^{11,12} Within this frame, in the recent years, the market needs have been pushing toward the design and the production of innovative packaging solutions. One of the proposed approaches is the combination of aluminium traditional layers with active polymeric coatings, capable of protecting aluminium from the action of agents coming from the foodstuff and, at the same time, improving the food quality, also preventing any contamination risk.¹³ Aluminium foils coated with antibacterial or antioxidant compounds play a fundamental role in extending the shelf-life of ready-to-eat food products improving the quality and safety of the food products.^{1,14} For this reason, the

application of multilayer materials is not only driven by the necessity to avoid toxicological effects, but also by the designing requirement of a single packaging configuration, which combines different properties and functions.

In the present study, we report the incorporation of a natural antimicrobial compound, namely eugenol, into a polymeric vinyl resin, to coat aluminium foils by means of a solvent casting technique to obtain an active material, potentially capable of extending shelf-life and quality of packaged foodstuff. The innovative approach is represented by the encapsulation of the active compounds into a porous inorganic nanocarriers which generally provide both the controlled release of the antimicrobial/antioxidant and its protection toward UV and/or solvents. This is considered an effective approach to enhance the efficiency of the active packaging materials, thus holding the quality of foods during storage.¹⁵ Mesoporous silica and natural halloysite are very attractive materials, since they can be used as nanocarriers which allow to embed active molecules in internal porosity both to preserve their specific activity and to control their release by pore architecture, pore size and specific molecule/pore wall interactions.^{16,17} In this work, eugenol, free and loaded into Santa Barbara Amorphous (SBA)-15 mesoporous silica, has been filled into the polymeric vinyl resin. The eugenol effect and dispersion on the structural and functional properties of the manufactured materials has been investigated. Moreover, the antimicrobial activity of the manufactured coatings has been evaluated against three foodborne pathogens, *Staphylococcus aureus*, *Escherichia coli* and *Pseudomonas aeruginosa* and three food spoilage bacteria, *Shewanella putrefaciens*, *Brochothrix thermosphacta* and *Lactobacillus plantarum*, following the procedure reported in the ISO 22196.

2 | MATERIALS AND METHODS

2.1 | Reagents

For the design of the active coating with antibacterial action, a solvent-based vinyl resin was used. Eugenol (EG-purity $\geq 99\%$), used as active compound, was purchased by Sigma Aldrich. Santa Barbara Amorphous (SBA)-15 mesoporous silica was supplied by ACS Material (Stock #SBA-15-8-20 g, maximum dimension of the single particles is about 1 μm , pore diameter 8–9 nm).

2.2 | Impregnation of SBA-15 loaded with eugenol

SBA was impregnated with eugenol, by using the following procedure. Known amount of eugenol was dissolved in

ethanol (5 ml per gram of substrate) for 15 min under stirring; subsequently, a suitable amount of mesoporous SBA-15 was added, and hold stirred for 30 min. The solid powder was dried at 35°C for 5 h under vacuum, obtaining a slightly yellow powder. During the filling process, eugenol/mesoporous silica weight ratio was equal to 0.71, chosen as optimal value allowing the maximum eugenol amount to fill the hosting SBA-15 total pore volume. The attained loaded sample was coded as SBA15_{EG}.

2.3 | Active coating preparation

Vinyl resin (VIN)-based coatings containing free eugenol (EG) and SBA15 containing (SBA15_{EG}) were deposited on flexible aluminium foils to obtain the active material, by using the following procedure. In a first case, completely free eugenol (5% wt/wt respect to the resin mass) and, in a second case, the combination of free eugenol (2.5% wt/wt) plus SBA-15 containing eugenol (2.5% wt/wt) were added to the vinyl resin to obtain the two coating formulations. In order to provide a homogenous distribution of the filler within the resin, it was stirred for 30 min at 1200 rpm and methyl ethyl ketone (MEK) was used to adjust the viscosity. Samples were coded as 5% EG and 5% (EG/SBA15_{EG}), respectively.

Subsequently, pristine resin, resin containing 5% EG and resin containing 5% (EG/SBA15_{EG}) were cast onto aluminium foils (thickness 12 µm), by means of a bar coater (K101 CONTROL COATER, by URAI, Italy, characterized by a spreadable surface of 170 x 250 mm and a variable speed range of 2 to 15 m/min). All the coated aluminium foil samples were dried at 80°C for 20 s. Then, in order to determine the weight of the coating and to verify the achievement of the desired coating value (10 ± 2 g/m², after drying), a 10 cm x 10 cm sample was cut and weighed before and after the removal of the coating with MEK solvent. The obtained samples have been coded: Al/VIN, Al/VIN/5%EG, Al/VIN/5%(EG/SBA15_{EG}).

2.4 | Experimental

2.4.1 | Powder and coating characterization

N₂ adsorption/desorption analyses were performed at 77 K by a Micromeritics ASAP 2020. The as-purchased SBA-15 samples were degassed at 150°C for 10 h. To measure specific surface areas, the BET method was employed, while pore size distribution evaluation was assessed by applying the BJH method considering only adsorption branches of the isotherms.

Thermogravimetric analysis (TGA) was carried out by using a TA Instruments Q500 apparatus. The samples were heated over the temperature range from 40°C to 900°C at a rate of 10°C min⁻¹ in an oxygen atmosphere.

The morphological analysis of neat and loaded vinyl coatings, as well as the aluminium thickness was evaluated by using a FEI Quanta 200 FEG scanning electron microscope (ESEM) (FEI, Eindhoven, The Netherlands) in high vacuum mode at an accelerating voltage within 10–20 kV range and a secondary electron detector (Everhart–Thornley detector). Before the observation, dried specimens were coated with an Au-Pd alloy by a sputter coater (Emitech K575, UK).

FTIR spectra were recorded, from 400–4000 cm⁻¹ with 4 cm⁻¹ resolution and 64 scans, at room temperature by a Nicolet FT-IR spectrometer (Thermo Scientific, Italy) in Attenuated Total Reflectance (ATR) mode.

Contact angle measurements were evaluated according to ASTM D7334 Standard Practice for Surface Wettability of Coatings,¹⁸ Substrates and Pigments by using a DataPhysics OCA 20 apparatus, by dripping distilled water onto at least ten different sites on each coated sample and the static contact angle was reported as the average from the measured values.

Electrochemical Impedance Spectroscopy Analysis has been performed by using a Gamry Instrument to evaluate the corrosion resistance of coatings. Impedance spectroscopy is an alternating frequency (AC) electrochemical technique. In particular, through an analysis of the impedance modulus and the phase angle, as a function of the frequency (Bode diagrams), impedance spectroscopy can give information on (i) defects in the organic coating, (ii) the progress of the corrosion, (iii) the functionality of the conversion layer.

2.4.2 | Evaluation of antibacterial effectiveness of active coatings

ISO-22196 (Plastics – Measurement of Antibacterial Activity on Plastics Surfaces)¹⁹ was used to measure the antibacterial activity of samples against *E. coli* (ATCC 13762), *P. aeruginosa* (ATCC 9027), *S. aureus* (ATCC 6538), *Shewanella putrefaciens* (ATCC 8071), *B. thermosphacta* (ATCC 11509) and *Lactobacillus plantarum* (WCFS 1). Bacterial growth was performed according to Orlo et al., 2021,²⁰ and flat and square (50 ± 2) x (50 ± 2) mm (maximum of 10 mm in thickness) specimens were prepared of each coating. Samples consisted of treated vinyl coatings containing free eugenol (EG) or SBA15 eugenol loaded (SBA-15_{EG}), while negative controls consisted of untreated vinyl coatings. Before the beginning of the test, all specimens were immersed in

70% ethanol, placed in Petri dishes and then inoculated with bacteria (0.4 ml suspension, with a final concentration of 6×10^5 cells/ml) from overnight cultures diluted with 1/500 Nutrient Broth. The test inocula were covered with a piece of disinfected polyethylene film ($(40 \pm 2) \times (40 \pm 2)$ mm and dipped in 70% ethanol). The inoculated samples were incubated at a specific growth temperature for each microbial strain and at a humidity condition of 90% for 24 h. After the incubation time, each sample was washed using soybean casein digest broth with lecithin and polyoxyethylene sorbitan monooleate (SCDLP) (10 ml). From this solution, serial dilutions were made 10 times in 1/800 phosphate buffer solution and each dilution (1 ml) as well as SCDLP (1 ml) recovered from the test sample were placed in duplicate in Petri dishes together with de Man, Rogosa and Sharpe agar (15 ml) for counting *L. plantarum* or plate count agar (15 ml) for counting *S. aureus*, *E. coli*, *P. aeruginosa*, *B. thermosphacta* and *S. putrefaciens*. Petri dishes were inverted and incubated at $30 \pm 1^\circ\text{C}$ (*L. plantarum*), $26 \pm 1^\circ\text{C}$ (*B. thermosphacta* and *S. putrefaciens*) and at $35 \pm 1^\circ\text{C}$ (*S. aureus*, *E. coli*, *P. aeruginosa*) from 40 to 48 h.

After incubation the number of viable cells was determined as follows:

$$N = \frac{100 \times C \times D \times V}{A} \quad (1)$$

where N is the number of viable bacteria recovered per cm^2 per test specimen, C is the average plate count for the duplicate plates, D is the dilution factor for the plates counted, V is the volume, in ml, of SCDLP added to the specimen, A is the surface area, in mm^2 , of the cover film. Then, the logarithmic value of the number of viable cells ($\text{Log}N$) was determined, and the antibacterial activity was expressed as R value²¹:

$$R = Ut - At \quad (2)$$

where Ut is the average of the common logarithm of the number of viable bacteria, in cells/cm^2 , recovered from the untreated test specimens after 24 h; At is the average of the common logarithm of the number of viable bacteria, in cells/cm^2 , recovered from the treated test specimens after 24 h.

2.5 | Statistical analysis

Each coating was tested in triplicate by performing three independent experiments. The statistically significant difference (unpaired t test) was evaluated between the $\text{Log}N$ values of the samples and those of the negative controls

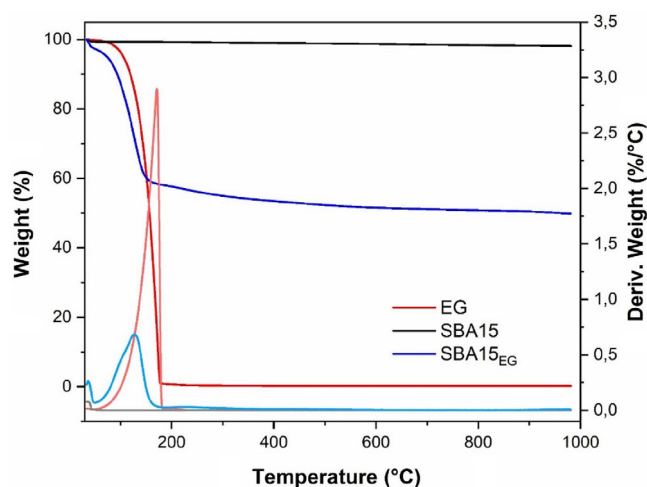


FIGURE 1 TGA (dark) and DTGA (light) curves of pristine eugenol (red), non-impregnated (black) and eugenol-loaded (blue) SBA15 [Color figure can be viewed at [wileyonlinelibrary.com](https://onlinelibrary.wiley.com/doi/10.1002/app.53519)]

(untreated specimens) by using Prism 5 analysis. Differences were considered significant for $*p < 0.05$, $**p < 0.01$ and $***p < 0.0001$.

3 | RESULTS AND DISCUSSION

3.1 | Powder and coating characterization

In order to evaluate the mesoporous silica loading capacity and the suitable eugenol amount for the SBA15 micro-pore filling, specific surface areas, pore size distributions, total pore volume and diameter of non-impregnated SBA15 were determined by applying both the BET and the BJH method. The obtained N_2 adsorption/desorption curves correspond to a type IV isotherm with an increase of N_2 adsorbed amount at relative pressures >0.5 . The specific SBA15 surface area was $445 \text{ m}^2/\text{g}$ and the corresponding pore diameter was 8.4 nm, while the total pore volume was $0.67 \text{ cm}^3/\text{g}$.¹⁶ This means that if this volume is completely filled with eugenol, it is possible to load about 0.71 g of eugenol per gram of hosting mesoporous silica. To estimate the real loading capacity after impregnation procedure, thermogravimetric analysis was carried out and the corresponding TGA-DTGA curves of pristine eugenol, non-impregnated and eugenol loaded SBA15 are reported in the Figure 1. The non-impregnated SBA15 curve highlighted a negligible weight loss due to the thermal decomposition of the organic groups onto the pore channels' walls. As all the samples show a constant weight loss at 900°C unaffected by the eugenol loading into the pores, it is possible to evaluate

FIGURE 2 SEM micrographs @200 μm magnitude (surface) of Al/VIN/5%EG and Al/VIN/5%(EG/SBA15_{EG}) samples

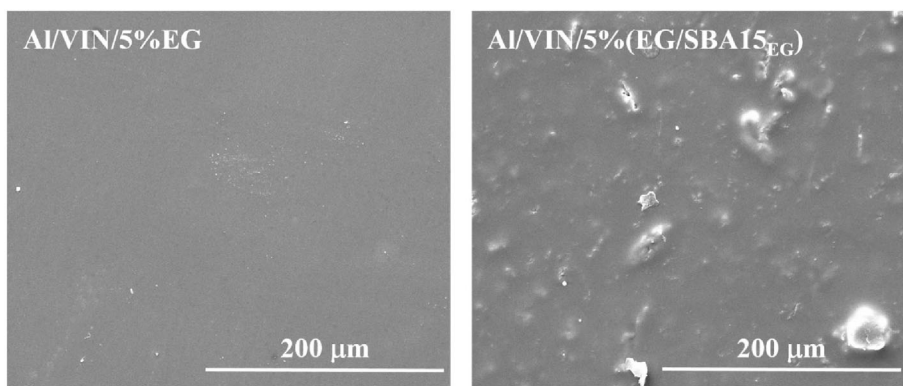
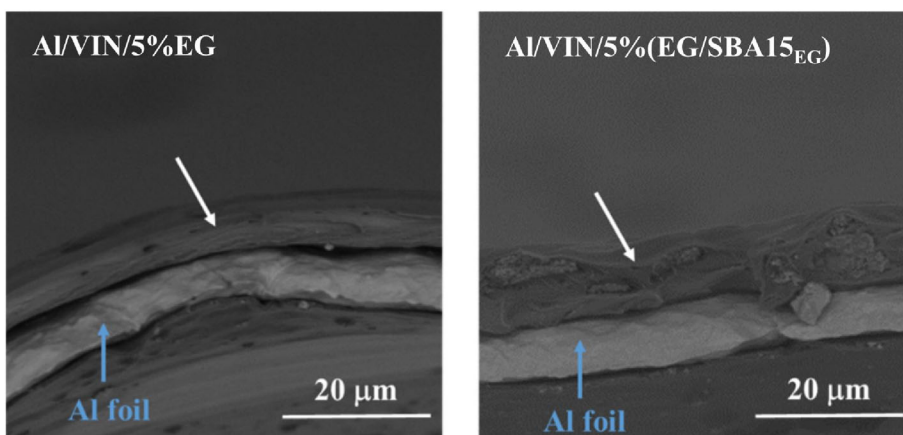


FIGURE 3 SEM micrographs @20 μm magnitude (section) of Al/VIN/5%EG and Al/VIN/5%(EG/SBA15_{EG}) samples. [Color figure can be viewed at wileyonlinelibrary.com]



the active compound content, EG (%), by using the following formula:

$$EG\% = W^{SBA} - W^{SBA/EG} \quad (3)$$

where W^{SBA} and $W^{SBA/EG}$ are respectively the neat and eugenol-loaded mesoporous silica residual percentage at 900°C. Computing the previous equation with the corresponding values, the final eugenol content percentage results of about 48% wt/wt. The attained results correspond to eugenol/silica weight ratios used during the impregnation process and they lead to the final achievement of an optimal effectiveness in loading antioxidant molecules within the pores of the selected mesostructures.²² However, the further potential location of eugenol on the outer surface of the silica mesoporous structure cannot be completely excluded.

SEM investigations were performed to evaluate the effect of EG and SBA15_{EG} fillers on the coating superficial morphology, as well as filler dispersion and coating thickness. SEM micrographs are shown in Figures 2 and 3. In Figure 2 it can be observed that the EG filler is well dispersed within the hosting polymer matrix, thus the surface coating of the Al/VIN/5%EG sample is characterized by a smooth surface. While for the Al/VIN/5%

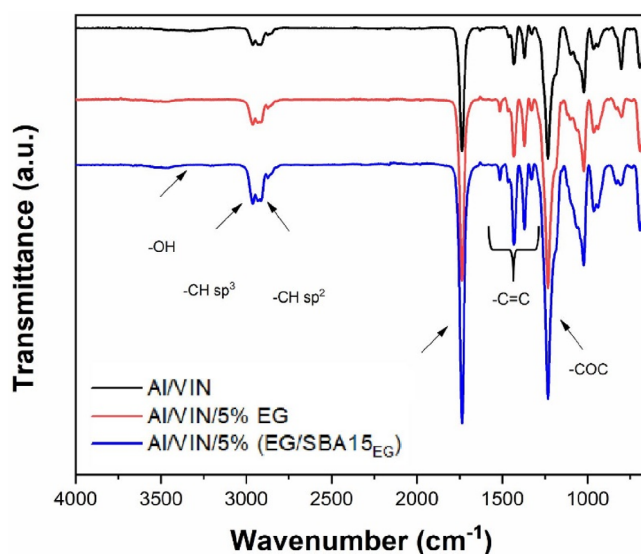


FIGURE 4 FTIR-ATR spectra of Al/VIN, Al/VIN/5%EG and Al/VIN/5%(EG/SBA15_{EG}) samples [Color figure can be viewed at wileyonlinelibrary.com]

(EG/SBA15_{EG}) samples, it is possible to note some SBA15 particles aggregation which determines a rougher and slightly bumpy surface of the final coatings. This will surely affect the final thickness as already reported in

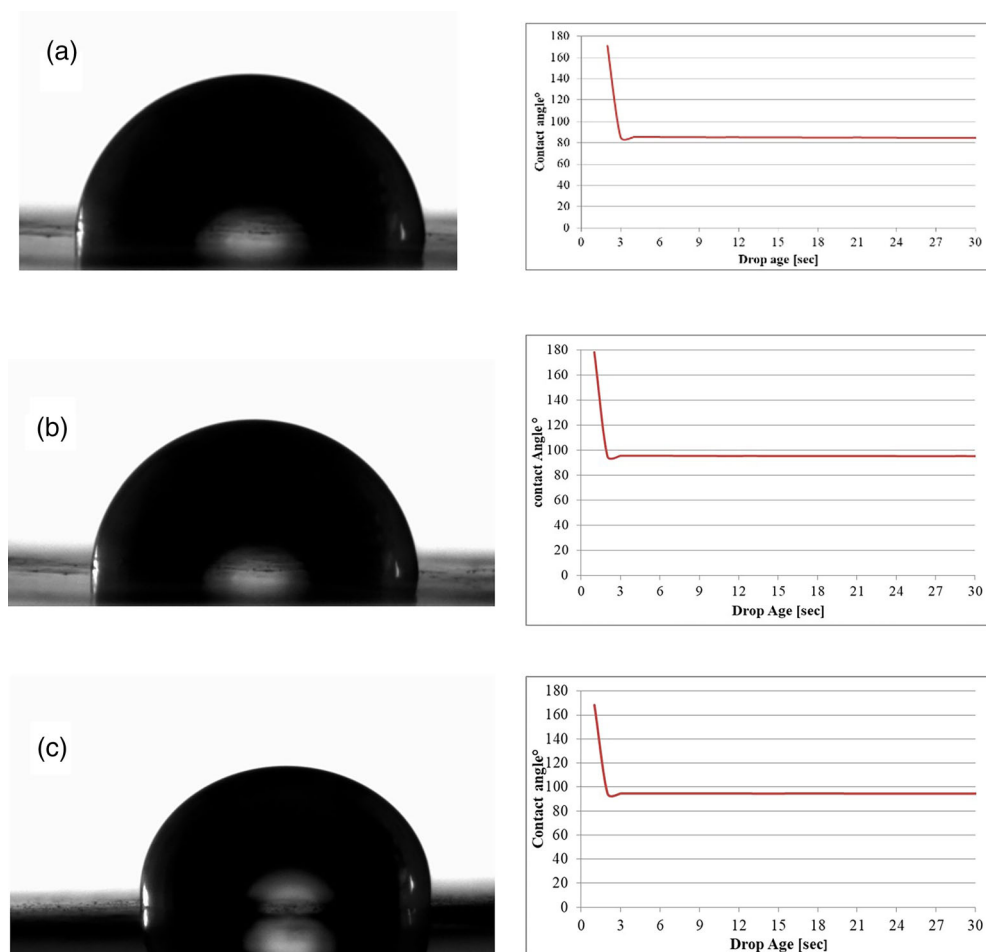


FIGURE 5 Image of drop angle and plot of variation contact angle from deposition of drop on coating for 30 s for Al/VIN (a), Al/VIN/5%EG (b) and Al/VIN/5%(EG/SBA15_{EG}) (c) [Color figure can be viewed at wileyonlinelibrary.com]

TABLE 1 Water contact angle values and drop images of the Al/VIN, Al/VIN/5%EG and Al/VIN/5%(EG/SBA15_{EG}) samples

Samples	Contact angle (°)
Al/VIN	85.00 ± 1.6
Al/VIN/5%EG	96.13 ± 1.0
Al/VIN/5%(EG/SBA15 _{EG})	96.26 ± 1.0

Figure 3, moreover the uneven surface due to the eugenol-filled SBA15 could lead to a weakening of the coating/metal interface in some places.

Moreover, the SEM micrographs of Figure 3 show that the thickness of the VIN/5%EG and VIN/5%(EG/SBA15_{EG}) coatings are 4.0 μm and 5.4 μm, respectively. Most likely, the highest thickness in the VIN/5%(EG/SBA15_{EG}) coating is due to the volume effect of some SBA15 particles.

A qualitative analysis of chemical properties of Al/VIN, Al/VIN/5%EG and Al/VIN/5%(EG/SBA15_{EG}) coatings was performed by FT-IR to investigate the potential interfacial interaction in the eugenol-loaded coatings compared to the neat vinyl resin (Figure 4).

The Al/VIN blank coating (black spectrum) shows all the FT-IR characteristic bands of vinyl resin. In details, the valence vibrations due to -OH and the ester carbonyl groups were observed at 3378 cm⁻¹ and 1727 cm⁻¹, respectively. The other two peaks, localized at 2877 cm⁻¹ and 2819 cm⁻¹ are ascribed to stretching vibration of -CH₂ and -CH₃ groups, respectively.^{23,24} In eugenol-loaded samples, an increase of the absorption bands at wavelengths of about 2877 cm⁻¹ and 2819 cm⁻¹ was observed, likely related to -CH carbon atoms with sp² and sp³ hybridization, respectively.^{25–27} All the peaks within the 720–1250 cm⁻¹ region are related to the presence of -C=C- carbon atoms, whereas sharp peaks in the range of 1500–1400 cm⁻¹ could be associated to -C=C- stretching of the aromatic moieties²⁸ characteristic of eugenol. As revealed by the absence of new evident peaks, both the eugenol-loaded samples show no chemical interaction with the vinyl resin. However, EG and SBA15_{EG} addition leads to an intensification of all Al/VIN characteristic peaks, likely related to the presence of the -C=O and -CH₂ functional groups.

Contact angle measurements were performed to investigate the water affinity of the pristine and eugenol

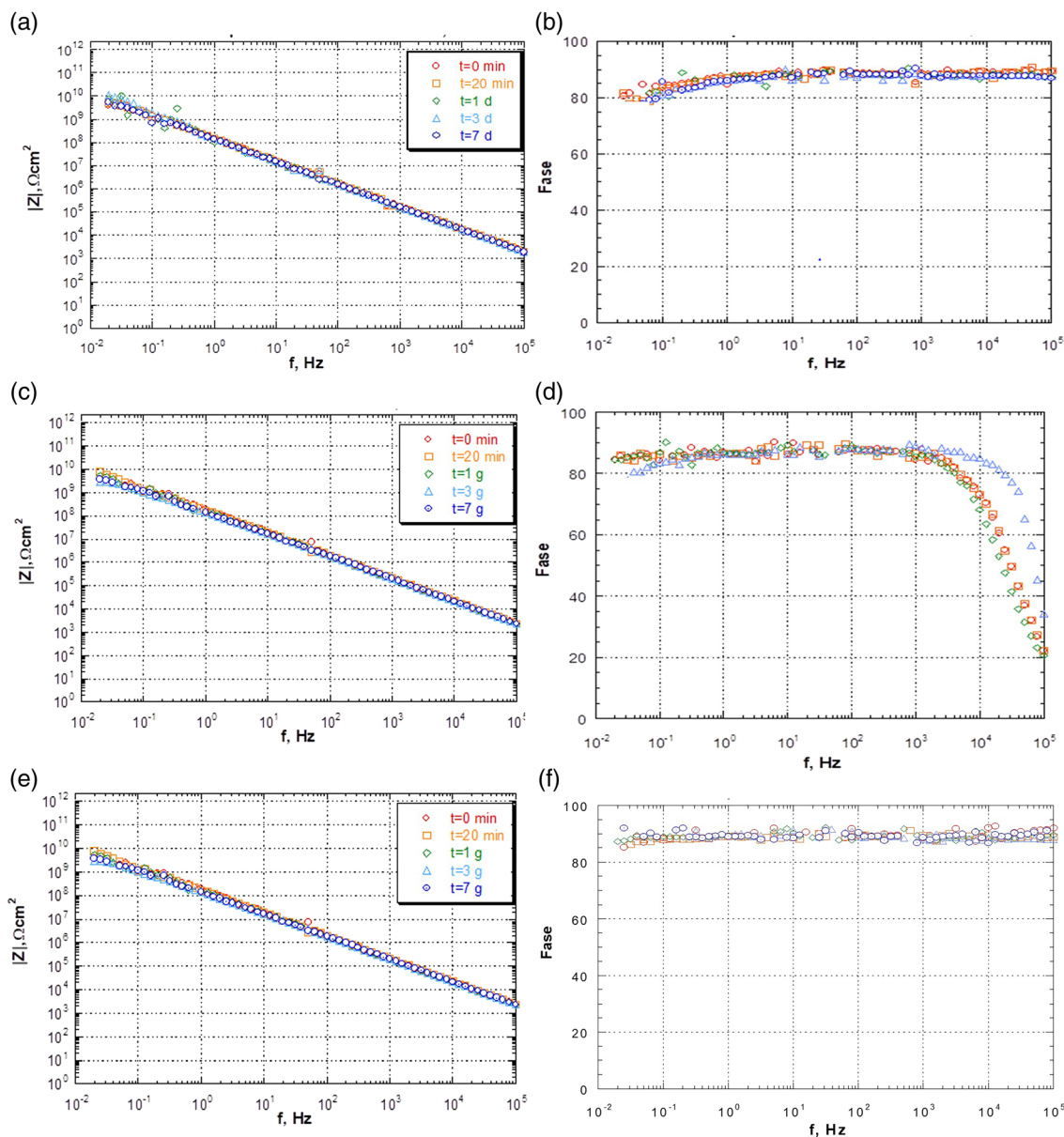


FIGURE 6 Electrochemical impedance module and phase angle in aerated aqueous solution of NaCl (3.5% wt/wt) of Al/VIN (a, b), Al/VIN/5%EG (c, d) and Al/VIN/5%(EG/SBA15_{EG}) (e, f) [Color figure can be viewed at [wileyonlinelibrary.com](https://onlinelibrary.wiley.com/doi/10.1002/app.53519)]

loaded vinyl resin. ASTM D7334-08 was used to evaluate the contact angle within 30 seconds after the deposition of the drop on the sample substrate. The value of the angle at time zero is relative to the drop immediately before deposition (Figure 5, inset graph). The obtained contact angle values and drop images are reported in Table 1 and Figure 5, respectively.

It is worth noting that water contact angle values for Al/VIN/5%EG and Al/VIN/5%(EG/SBA15_{EG}) are respectively 96.13° and 96.26°, thus showing a more hydrophobic character compared to the neat vinyl resin-based coating (85°). It has been already proved that the presence of eugenol increases the hydrophobicity of the

materials²⁹ and this is an interesting and good result since materials with high contact angle allow for prolonged release of antimicrobial agents and, also, as reported by Huhtamäki et al.,³⁰ lead to increased shelf-life of meat products and allow to avoid the adhesion of bacteria to the surface of materials.³¹ Furthermore, the enhanced hydrophobic property of eugenol-filled vinyl resin could facilitate its potential application in active food packaging field due to the better water-resistance function to prevent moisture alter the material structure.³²

In order to investigate the potential use as packaging materials, electrochemical impedance spectroscopy (EIS)

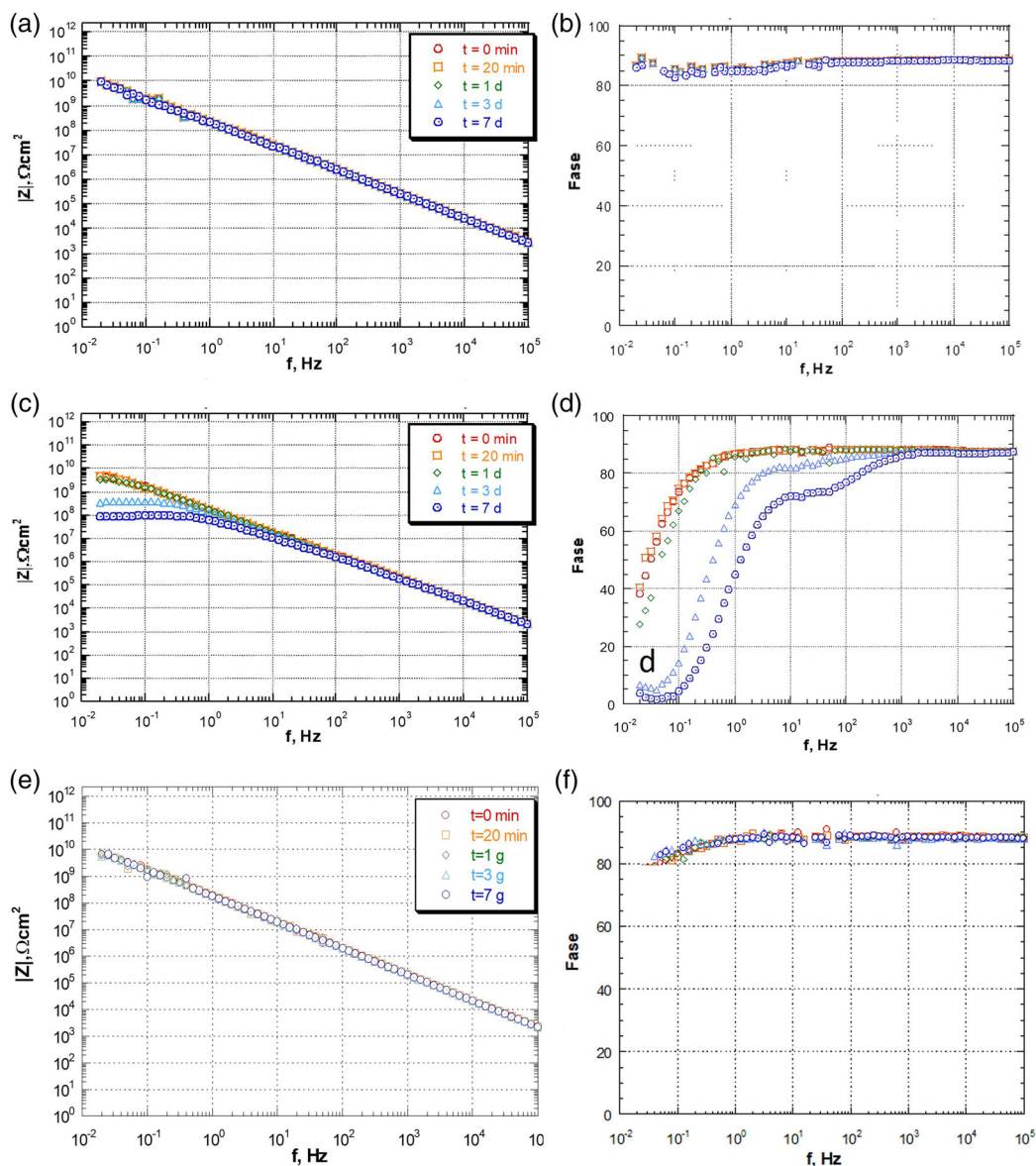


FIGURE 7 Electrochemical impedance module and phase angle in aerated aqueous solution of lactic acid pH 4 of Al/VIN (a, b), Al/VIN/5%EG (c, d) and Al/VIN/5%(EG/SBA15_{EG}) (e, f) [Color figure can be viewed at [wileyonlinelibrary.com](https://onlinelibrary.wiley.com/doi/10.1002/app.53519)]

was used to evaluate the corrosion resistance to acidic and salty foods of the developed materials. An acidic solution (pH 4) and a sodium chloride solution (3.5% wt/wt) were used to simulate acidic and salty foods, respectively. Thus, EIS analysis has been performed by bringing in contact the coatings with an aqueous solution of sodium chloride 3.5% wt/wt and with an aqueous solution of lactic acid pH 4.³³ Impedance and angle phase values are reported in Figures 6 and 7 respectively.

In Figure 6, results show that in both coatings the impedance exhibits very high values ($10^{10} \Omega\text{cm}^2$) and the phase angle is constant after 7 days, thus showing the absence of any corrosion phenomenon. For sample

Al/VIN/5%EG (Figure 6d), the observed curve variation in the frequency range between 10^5 – 10^3 Hz phase angle is due to the porosity of the system which allows the diffusion of the NaCl solution within the coating. Results reported in Figure 7 show that the coating Al/VIN/5%(EG/SBA15_{EG}) does not show corrosion phenomena neither in contact with an aqueous solution of lactic acid pH 4, whereas Al/VIN/5%EG sample exhibits corrosion phenomenon likely due to a sort of induced porosity caused by the eugenol leaching into the aqueous solution, in fact in Figure 7c, it can be observed a change of curvature correlated to the first time constant τ_1 at high frequencies at day seven.

FIGURE 8 Logarithmic values of viable cell numbers (LogN) of *E. coli*, *P. aeruginosa*, *S. aureus*, *B. thermosphacta*, *L. plantarum* and *S. putrefaciens* were recovered from neat Al/VIN coatings (NC) and from Al/VIN/5%EG and Al/VIN/5%(EG/SBA15_{EG}) after 24 h of exposure. The results are expressed as $\overline{\text{LogN}} \pm \text{SD}$ ($n = 3$). Asterisks indicate the statistically significant difference between the samples and the negative control (* $p < 0.05$, ** $p < 0.01$, *** $p < 0.001$ - unpaired t test)

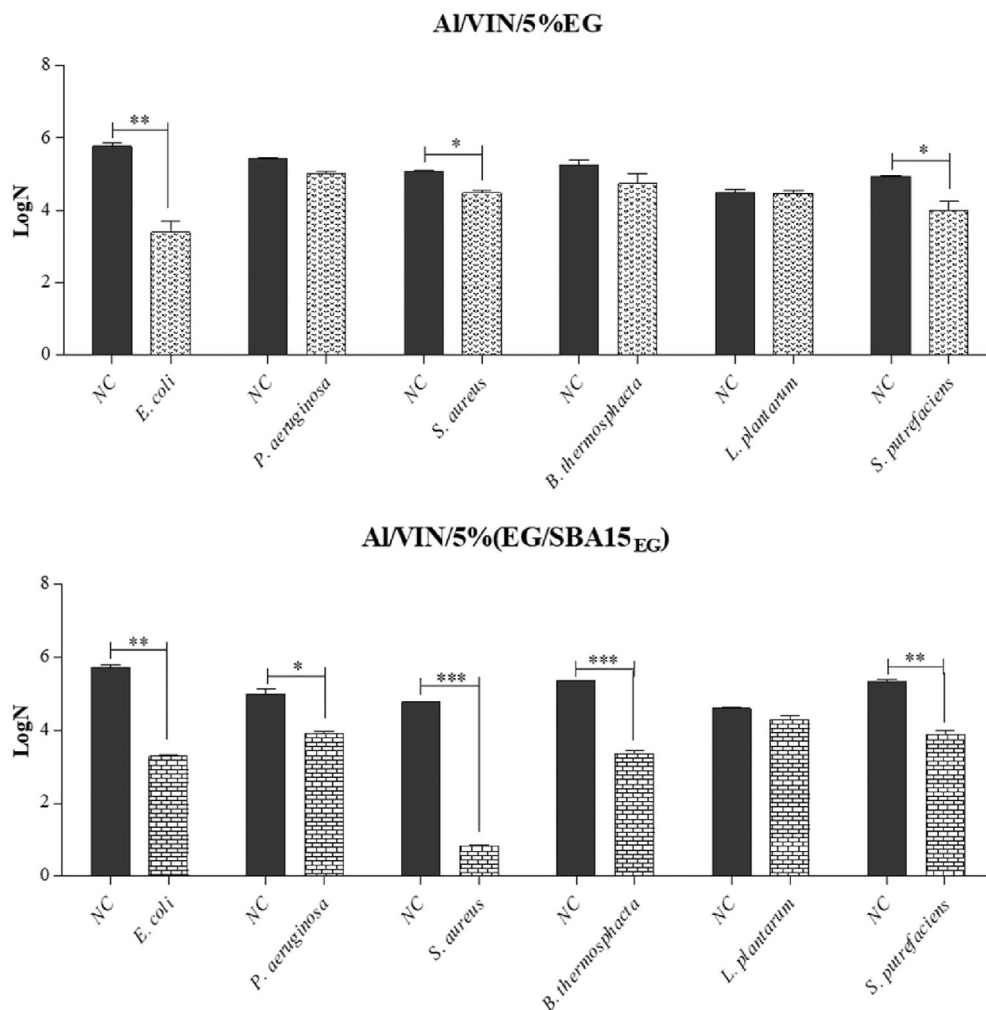


TABLE 2 The antibacterial activity expressed as \overline{R} values \pm standard deviation (SD) $n = 3$, obtained by Al/VIN/5%EG and Al/VIN/5%(EG/SBA15_{EG}) on *E. coli*, *P. aeruginosa*, *S. aureus*, *B. thermosphacta*, *L. plantarum* and *S. putrefaciens*.

Bacterial strains	R values	
	Al/VIN/5%EG	Al/VIN/5%(EG/SBA15 _{EG})
<i>E. coli</i>	2.36 \pm 0.21	2.41 \pm 0.05
<i>P. aeruginosa</i>	0.29 \pm 0.02	1.06 \pm 0.12
<i>S. aureus</i>	0.62 \pm 0.10	3.62 \pm 0.50
<i>B. thermosphacta</i>	0.51 \pm 0.13	1.98 \pm 0.07
<i>L. plantarum</i>	0.03 \pm 0.01	0.30 \pm 0.15
<i>S. putrefaciens</i>	0.94 \pm 0.27	1.46 \pm 0.08

3.2 | Antibacterial activity

For each active coating developed, the antibacterial activity was evaluated against *S. aureus*, *E. coli*, *P. aeruginosa*, *B. thermosphacta*, *L. plantarum* and *S. putrefaciens* using ISO-22196 (Plastics – Measurement of Antibacterial Activity on Plastics Surfaces). The results of the antimicrobial activity of Al/VIN/5%EG and Al/VIN/5%(EG/SBA15_{EG}) were shown in Figure 8.

Results highlighted that a significant reduction of *S. aureus* and *E. coli* viable cells (compared to the relative

NC) was induced when they were exposed to Al/VIN/5%EG, with p values less than 0.01 and 0.05, respectively. On the other hand, among all the selected food spoilage bacterial strains, only *S. putrefaciens* viability was significantly affected by Al/VIN/5%EG. Interestingly, when eugenol was loaded in SBA15 mesoporous silica nanoparticles and embedded into the vinyl resin, not only its antibacterial efficacy significantly increased on *S. aureus* and *S. putrefaciens*, but it also affected *P. aeruginosa* (* $p < 0.05$) and *B. thermosphacta* (*** $p < 0.001$) viability. The advantages of loading eugenol in SBA15 in increasing

the antibacterial activity of the free eugenol are even more evident from the results expressed in terms of R (meant as log microbial growth reduction), as reported in Table 2.

R values were obtained from the difference between the logarithms of the viable cells recovered from the treated and untreated coatings. According to Scuri et al.,³⁴ the R value may be used to identify the efficacy of an antibacterial material using the following classification:

- $R \leq 0.5$ = no antimicrobial activity;
- $0.5 \leq R \leq 1$ = slight antimicrobial activity;
- $1 < R \leq 2$ = medium antimicrobial activity;
- $2 < R < 3$ = good antimicrobial activity;
- $R > 3$ = very good antimicrobial activity.

The highest R values were obtained using Al/VIN/5% (EG/SBA15_{EG}) on foodborne pathogens with the greatest effect on *S. aureus* ($R = 3.62$).

Basically, the use of the inorganic (nano)carrier helps to control the transport of active compounds throughout the bacterial wall. Indeed, as reported by Wu et al.,³⁵ the encapsulation of curcumin in SBA15 leads to an improvement in its antibacterial efficacy on *S. aureus* with a greater effectiveness on *S. aureus* than *E. coli*, probably due to the difference in the cellular structure of the membrane of these bacterial species. Furthermore, as demonstrated by Memar et al.,³⁶ mesoporous silica nanoparticles, while not exerting their own significant antibacterial effect, could contribute to influencing the transport mechanisms of the cell membrane in microorganisms. Indeed, Gámez et al.³⁷ noted that the encapsulation of natural compounds in SBA15 results in an increase in their solubility and chemical stability, also improving their bioavailability and efficacy against pathogens. In line with the above results, the use of SBA15 as a carrier for eugenol resulted in an active coating exhibiting (i) an antimicrobial activity superior to that of the free eugenol-containing coating on all bacterial strains studied, (ii) good antimicrobial activity against *E. coli* and (iii) very good antimicrobial activity against *S. aureus*.

According to Torlak and Sert,³⁸ there are two types of mechanisms by which active coatings can act: contact of bacterial cells with the functional groups of compounds responsible for antimicrobial activity in the coatings, and release of water-soluble active compounds from the coating into liquid solution containing bacterial cells.

Since eugenol is not a water-soluble molecule, the activity of the tested coatings may be related to the first mechanism. In fact, in recent literature, several works are reported on the use of eugenol for the production of active food packaging. Sanahuja and García³⁹ obtained active packaging films through the incorporation of pure

eugenol in different polymeric matrices such as low density polyethylene, polyethylene terephthalate, poly lactic acids. Furthermore, Li et al.³² tested eugenol in poly lactic acid films recording good antibacterial property against *S. aureus* and *E. coli* and demonstrating its potential use for active food packaging. Moreover, Meléndez-Rodríguez et al.⁴⁰ developed antimicrobial films of 3-hydroxybutyrate-co-3-hydroxyvalerate using mesoporous silica supports for eugenol and, among the different microbial species used, obtained the best antimicrobial activity against *S. aureus*. To the best of our knowledge there are no data in the literature on the antibacterial activity of materials containing eugenol against *B. thermosphacta*, *S. putrefaciens* and *L. plantarum*. However, in the present study, *L. plantarum* was the only strain that was not susceptible to both coatings. The antibacterial efficacy of eugenol against food spoilage bacteria and foodborne pathogens was highlighted by Orlo et al.²⁰ Furthermore, these authors observed that various natural methoxyphenolic compounds, including eugenol, were poorly active against *L. plantarum* which is considered one of the main spoilage bacteria causing a decrease in the quality of food with discoloration, souring, slime formation, unpleasant aroma and gassing in food. However, the high resistance shown by *L. plantarum* to eugenol, free or loaded in SBA15, could be an additional advantage for applications of VIN/5%EG and VIN/5% (EG/SBA15_{EG}) coatings such as food packaging. Hence, lactobacilli can not only inhibit the growth of harmful microorganisms through competition for nutrients,⁴¹ but could also be used as starters in dairy products and some processed meats to provide acidity, contribute to flavor and produce antimicrobial compounds (e.g., bacteriocins, peroxide) that promote food preservation.⁴² Therefore, the designed materials could be used for the packaging of fresh meats and cheeses which are considered highly perishable foods that require new strategies to extend their shelf-life.

4 | CONCLUSION

In this paper eugenol, a natural antimicrobial compound, has been successfully incorporated in a polymeric vinyl resin and used for the first time to coat aluminium foils by means of a solvent casting technique to obtain an antimicrobial material potentially capable to extend the shelf-life and quality of packaged foodstuff. Structural, thermal, morphological and functional properties of the composite coating were investigated examining the effect of dispersing the eugenol (i) freely directly into the resin and (ii) loaded into the nanochannel of a mesoporous silica, the SBA15.

The TGA assessed that the eugenol amount, was about 48%, as computed by a model calculation implemented taking into account the density of pores. FTIR analysis highlighted that both EG and SBA15_{EG} show no chemical interaction with the vinyl resin, however, their addition leads to an intensification of all Al/VIN characteristic peaks, likely related to the presence of the -C=O and -CH₂ functional groups. By water contact angle measurements, eugenol based-materials shown a higher hydrophobicity (>90°) compared to the pristine vinyl coating (85°). Electrochemical impedance spectroscopy highlighted no corrosion phenomena of the VIN/5%EG/SBA15_{EG} coating and corrosion phenomena of the VIN/5%EG coating after 7 days of exposure to lactic acid pH = 4. Regarding antibacterial efficacy, the VIN/5% (EG/SBA15_{EG}) coating reduced the log of viable cells of the Gram-positive strains *S. aureus* and *B. thermosphacta* more than VIN/5%EG coating suggesting that SBA15 mesoporous silica could contribute to transport the active compound into the bacterial cell wall.

Future studies will focus on the antibacterial activity of the two active materials using real food systems in order to evaluate their potential ability to extend the shelf-life of food.

AUTHOR CONTRIBUTIONS

Elena Orlo: Data curation (lead); investigation (lead); methodology (lead); writing – original draft (lead). **Mariamelia Stanzione:** Data curation (lead); investigation (lead); methodology (lead); writing – original draft (lead). **Margherita Lavorgna:** Project administration (lead); supervision (lead); writing – review and editing (lead). **Marina Isidori:** Conceptualization (lead); supervision (lead); writing – review and editing (lead). **Aldo Ruffolo:** Data curation (lead); investigation (lead); methodology (lead); writing – original draft (lead). **Ciro Sinagra:** Project administration (lead); supervision (lead); writing – review and editing (lead). **Giovanna Giuliana Buonocore:** Conceptualization (lead); project administration (lead); writing – review and editing (lead).

ACKNOWLEDGMENT

Technical support of Mrs. A. Aldi and Mrs. M.R. Marcedula is kindly acknowledged. Elena Orlo and Mariamelia Stanzione have contributed equally to this work and they share first authorship.

DATA AVAILABILITY STATEMENT

Supporting data for this experimental work will be available from the corresponding author upon reasonable request.

ORCID

Giovanna G. Buonocore  <https://orcid.org/0000-0002-4033-0624>

REFERENCES

- [1] H. Dogan, M. Koral, Y. İ. Tülay, *J. Plast. Film Sheeting* **2009**, 25, 207.
- [2] N. N. de Kruijf, M. van Beest, R. Rijk, T. Sipilainen-Malm, L. P. Paseiro, B. De Meulenaer, *Food Addit. Contam.* **2002**, 19, 144.
- [3] C. Nerin, in *Oxidation in Foods and Beverages and Antioxidant Applications*, Vol. 2 (Eds: E. A. Decker, R. J. Elias, D. J. McClements), Woodhead, Cambridge, United Kingdom **2010**, Ch. 16. <https://doi.org/10.1533/9780857090331.3.496>
- [4] L. J. Bastarrachea, D. E. Wong, M. J. Roman, Z. Lin, J. M. Goddard, *Coatings* **2015**, 5, 771.
- [5] K. Bentayeb, C. Rubio, R. Batlle, C. Nerin, *Anal. Bioanal. Chem.* **2007**, 389, 1989.
- [6] P. Lopez, C. Sanchez, R. Batlle, C. Nerin, *J. Agric. Food Chem.* **2007**, 55, 8814.
- [7] C. Nerin, L. Tovar, J. Salafranca, *J. Food Eng.* **2008**, 84, 313.
- [8] C. Exley, *Environ. Sci.* **1807**, 2013, 15.
- [9] T. Stahl, S. Falk, A. Rohrbeck, S. Georgii, C. Herzog, A. Wiegand, S. Hotz, B. Boschek, H. Zorn, H. Brunn, *Environ. Sci. Eur.* **2017**, 29, 19.
- [10] T. Stahl, S. Falk, H. Taschan, B. Boschek, H. Brunn, *Eur. Food Res. Technol.* **2018**, 244, 2077.
- [11] S. Maya, T. Prakash, K. D. Madhu, D. Goli, *Biomed. Pharmacother.* **2016**, 83, 746.
- [12] C. Exley, E. Clarkson, *Sci. Rep.* **2020**, 10, 7770.
- [13] A. Gisario, C. Aversa, M. Barletta, S. Natali, F. Veniali, *Opt. Laser Technol.* **2021**, 142, 107237.
- [14] H. Cui, J. Wu, C. Li, L. Lin, *LWT-Food Sci. Technol.* **2017**, 81, 233.
- [15] A. Bahrami, R. Delshadi, E. Assadpour, S. M. Jafari, L. Williams, *Adv. Colloid Interface Sci.* **2020**, 278, 102140.
- [16] M. Stanzione, N. Gargiulo, D. Caputo, B. Liguori, P. Cerruti, E. Amendola, M. Lavorgna, G. G. Buonocore, *Eur. Polym. J.* **2017**, 89, 88.
- [17] F. Tescione, G.G. Buonocore, M. Stanzione, M. Oliviero, M. Lavorgna, Controlling the release of active compounds from the inorganic carrier halloysite, in: AIP conference proceedings code 105839, vol. 1599, 2014, pp. 446–449. doi: <https://doi.org/10.1063/1.4876874>.
- [18] ASTM D7334 standard practice for surface wettability of coatings, substrates and pigments by advancing contact angle measurement.
- [19] ISO-22196: **2007**, Plastics–Measurement of antibacterial activity on plastics surfaces.
- [20] E. Orlo, C. Russo, R. Nugnes, M. Lavorgna, M. Isidori, *Foods* **1807**, 2021, 10.
- [21] S. Ghamrawi, J. P. Bouchara, O. Tarasyuk, S. Rogalsky, L. Lyoshina, O. Bulko, J. F. Bardeau, *Mater. Sci. Eng.* **2017**, 75, 969.
- [22] N. Gargiulo, I. Attianese, G. G. Buonocore, D. Caputo, M. Lavorgna, G. Mensitieri, M. Lavorgna, *Microporous Mesoporous Mater.* **2013**, 167, 10.
- [23] D. Rosu, C. N. Cascaval, L. Rosu, *E-Polym.* **2008**, 105, 1.
- [24] J. Chaudhary, S. Dadhich, S. Jinger, G. Tailor, *Int. J. Chem. Eng. Res.* **2017**, 9, 99.
- [25] S. C. Kuo, S. K. Chuang, H. Y. Lin, L. H. Wang, *Anal. Chim. Acta* **2009**, 653, 91.
- [26] M. Ginting, D. Surbakti, N. Triana, *Nat. Resour. J.* **2019**, 1, 31.

- [27] E. Makuch, A. Nowak, A. Günther, R. Petech, L. Kucharski, W. Duchnik, A. Klimowicz, *AMB Express* **2020**, *10*, 187.
- [28] K. Pramod, C. V. Suneesh, S. Shanavas, S. H. Ansari, J. Ali, *J. Anal. Sci. Technol.* **2015**, *6*, 34.
- [29] V. Navikaite-Snipaitiene, L. Ivanauskas, V. Jakstas, N. Rüegg, R. Rutkaite, E. Wolfram, S. Yilidrim, *Meat Sci.* **2018**, *145*, 9.
- [30] T. Huhtamäki, X. Tian, J. T. Korhonen, R. H. A. Ras, *Nat. Protoc.* **2018**, *13*, 1521.
- [31] A. K. Sri, P. Deeksha, G. Deepika, J. Nishanthini, G. S. Hikku, S. Antinate Shilpa, K. Jeyasubramanian, R. Murugesan, *J. Ind. Eng. Chem.* **2020**, *92*, 1.
- [32] M. Li, H. Yu, Y. Xie, Y. Guo, Y. Cheng, H. Qian, W. Yao, *LWT-Food Sci. Technol.* **2021**, *139*, 110800.
- [33] A. Amitrano, C. Salerno, C. Sinagra, *Verniciatura Industriale* **2012**, *534*, 640.
- [34] S. Scuri, F. Petrelli, I. Grappasonni, L. Idemudi, F. Marchetti, C. Di Nicola, *Acta Biomed.* **2019**, *90*, 370.
- [35] C. Wu, Y. Zhu, T. Wu, L. Wang, Y. Yuan, J. Chen, Y. Hu, J. Pang, *Food Chem.* **2019**, *288*, 139.
- [36] M. Y. Memar, M. Yekani, H. Ghanbari, S. Shahi, S. Sharifi, S. M. Dizaj, *Artif. Cells Nanomed. Biotechnol.* **2020**, *48*, 1354.
- [37] E. Gámez, H. Elizondo-Castillo, J. Tascon, S. García-Salinas, N. Navascues, G. Mendoza, M. Arruebo, S. Irusta, *Nanomaterials* **2020**, *10*, 616.
- [38] E. Torlak, D. Sert, *Int. J. Biol. Macromol.* **2013**, *60*, 52.
- [39] A. B. Sanahuja, A. V. García, *Polymer* **2021**, *13*, 1053.
- [40] B. Meléndez-Rodríguez, K. J. Figueroa-Lopez, A. Bernardos, R. Martínez-Máñez, L. Cabedo, S. Torres-Giner, J. M. Lagaron, *Nanomaterials* **2019**, *9*, 227.
- [41] N. Vieco-Saiz, Y. Belguesmia, R. Raspoet, E. Auclair, F. Gancel, I. Kempf, D. Drider, *Front. Microbiol.* **2019**, *10*, 57.
- [42] A. Djukic-Vuković, D. Mladenovic, B. Lakicevic, L. Mojovic, *IOP Conf. Ser. Earth Environ. Sci.* **2021**, *854*, 012025.

How to cite this article: E. Orlo, M. Stanzione, M. Lavorgna, M. Isidori, A. Ruffolo, C. Sinagra, G. G. Buonocore, M. Lavorgna, *J. Appl. Polym. Sci.* **2023**, *140*(9), e53519. <https://doi.org/10.1002/app.53519>